Appl Phys B (2010) 98: 647–652
DOI 10.1007/s00340-009-3858-4

Applied Physics B
Lasers and Optics

Solitonic eigenstates of the chaotic Bose–Hubbard Hamiltonian

H. Venzl · T. Zech · B. Oleś · M. Hiller · F. Mintert · A. Buchleitner

Received: 1 August 2009 / Revised version: 2 December 2009 / Published online: 24 December 2009

Abstract We study the evolving energy spectrum of interacting ultra-cold atoms in an optical lattice as a function of an external parameter, the tilt of the lattice. In a regime where the quantum mechanical model, the Bose–Hubbard Hamiltonian, shows predominantly chaotic behavior, we identify regular structures in the parametric level evolution and characterize the eigenstates associated with these structures. The mechanism generating these structures is found to be different from Stark localization or energetic isolation and is induced by an interplay of driving and interaction.

Understanding the transition from single-particle to many-body physics is one of the fundamental problems in quantum mechanics. With the advent of ultra-cold atoms trapped in optical lattices we have at our disposal a perfect test ground for such questions that were inaccessible to experiments until recently [1]. Namely, in modern lattice systems essentially all relevant parameters like the lattice configuration, the degree of disorder in the sample, and inter-particle interaction strength [2, 3] can be controlled extremely well in an experiment. For example, tuning the inter-atomic interaction strength [4, 5] allowed to observe the transition from a Mott-insulator state of strongly repulsive atoms to superfluid state of weakly interacting atoms [6]. In the former case, the ground state is essentially an eigenstate to the displacement operator (i.e., the uncertainty in the number of atoms per lattice site is small) while in the latter case, the ground state is essentially a momentum eigenstate.

However, it is not only the ground states that display interesting properties, but also excited states have caught attention: for example, tightly bound pairs of atoms were experimentally observed [7] in a regime with strongly repulsive inter-atomic interactions. The bonding, which at first sight appears rather counter-intuitive, is a result of the imposed lattice and can be understood in terms of energetic isolation. Due to the (strongly) repulsive on-site interaction the bound states lie energetically above the rest of the spectrum and hence there is no un-bound state to which a resonant transition would be possible. Experimentally, this has resulted in long life times and second order tunneling of the bound pairs.

The corresponding parameter regimes in which the dynamics is dominated by either interaction (Mott regime) or kinetic (superfluid regime) energy allow an analytical theoretical treatment. The situation gets significantly more complicated when the interaction energy is comparable to the single-particle kinetic energy. Then, the system can exhibit quantum chaos [8–11], leading to a sensitive dependence on the external conditions. The resulting complex dynamics is a serious challenge in any experiment and can render the atoms essentially uncontrollable. At the same time, it is known that on the transition from integrable to chaotic behavior not all regular structures in a classical system need be destroyed immediately [12]. Also quantum mechanical systems have been proven to display similar features and even enhanced robust structure like non-linear resonances [13], which open new paths for the control of chaotic systems. In this paper we will identify such regular structures that per-

H. Venzl (✉) · T. Zech · M. Hiller · F. Mintert · A. Buchleitner
Albert-Ludwigs-Universität Freiburg, Hermann-Herder-Str. 3, 79104 Freiburg, Germany
e-mail: hannah.venzl@physik.uni-freiburg.de

B. Oleś
Marian Smoluchowski Institute of Physics and Mark Kac Complex Systems Research Center, Jagiellonian University, Reymonta 4, 30-059 Kraków, Poland

sist well into the chaotic regime and describe the underlying mechanism that generates them.

Modeling The simplest non-trivial quantum model that describes N ultra-cold bosonic atoms stored in an optical lattice is the Bose–Hubbard Hamiltonian (BHH) [6]:

$$\hat{H} = -\frac{J}{2}\sum_{l=1}^{M-1}(\hat{a}_{l+1}^{\dagger}\hat{a}_l + h.c.) + \frac{U}{2}\sum_{l=1}^{M}\hat{n}_l(\hat{n}_l - 1) + F\sum_{l=1}^{M}\tilde{l}\hat{n}_l. \quad (1)$$

Here $\hat{a}_l$ ($\hat{a}_l^{\dagger}$) annihilates (creates) a particle in the Wannier state at the l-th site, $\hat{n}_l = \hat{a}_l^{\dagger}\hat{a}_l$ is the associated number operator, M specifies the number of lattice sites, $\tilde{l} = -M/2 + l$ for even M and $\tilde{l} = -(M-1)/2 + l$ for odd M. The control parameters J, U and F describe the strength of the single-particle tunneling, the on-site interaction, and the static field (e.g. tilting of the lattice under the influence of gravitation).[1]

The Bose–Hubbard model is based on a single (lowest) band approximation of the optical lattice [6]. This assumption holds provided that the kinetic energy, the interaction energy, and the local chemical potential (resulting from the tilt), are too low to excite states in higher Bloch bands. Therefore, the lattice must be very deep [6, 14] inducing large band gaps. Furthermore, the interaction energy has to be smaller than the single-particle ground-state energy, so as to not considerably modify the single-particle wave function. In the experiment, these conditions can be met since the control parameters are readily controlled [2]: while J and F are solely determined by the lattice geometry, the inter-atomic interaction U can additionally be adjusted using Feshbach resonances [15, 16].

If one of these three parameters is dominant the dynamics is governed by the corresponding term in the Hamiltonian (1). Accordingly, the dynamics is then regular and the system eigenstates are approximated very well by Bloch waves (for $J \gg U, F$), Mott-insulator states (for $U \gg J, F$) or Wannier–Stark states (for $F \gg J, NU$). The small terms of the Hamiltonian can be treated as perturbations and the system eigenfrequencies depend on these perturbations linearly. For $J \simeq U \gtrsim F$, the energy spectrum and hence the dynamics can become chaotic [10, 17, 18]. In contrast to the regular regime, here virtually all quantities show an extremely complicated dependence on the system parameters J, U and F.

[1] We note that the specific choice of $\tilde{l}$ corresponds to a tilting around the central lattice site but this has no further physical implications.

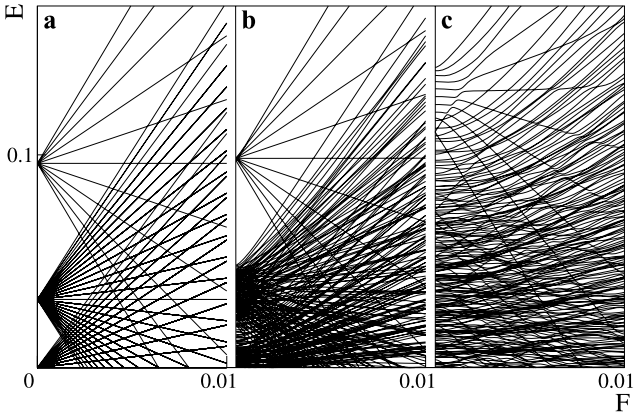

Fig. 1 Parametric level evolution: energy spectrum of the BHH equation (1) as a function of the tilting F for 3 bosons on 11 lattice sites for fixed on-site interaction $U = 0.032$; (**a**) no tunneling $J = 0$, (**b**) dominant interaction $U \gg J = 0.01$ and (**c**) chaotic regime $U \approx J = 0.038$

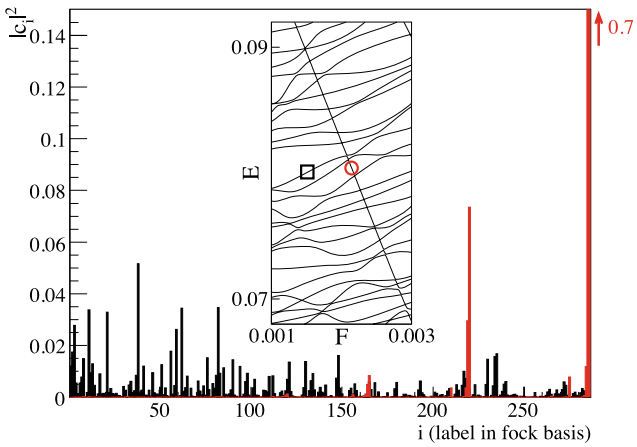

Fig. 2 Squared components of two eigenstates in the Fock basis. The *inset* shows a magnification of the parametric level evolution for the chaotic case (Fig. 1(c)). One sees one solitonic state going from the top to the bottom. The *red circle* marks the solitonic state, plotted gray in the component plot. The *black square* labels a random state of the chaotic background

Parametric level evolution In order to give an impression of how differently the energy spectrum behaves we plot in Fig. 1 the energy levels of the BHH as a function of the tilt F for 3 bosons on 11 lattice sites for fixed interaction $U = 0.032$ [19] and different values of the tunneling strength $J = 0$ (a), $J = 0.01$ (b), and $J \approx U$ (c). While for vanishing tunneling J (Fig. 1(a)) the spectrum is composed of intersecting straight lines, this situation changes drastically as J is increased (Fig. 1(b)). Finally, in panel (c) the bulk of the spectrum shows the above mentioned sensitivity to external conditions (in this case the tilt). Despite the chaoticity [19] in that regime, there are still several regular structures in the spectrum represented by (almost) straight lines; this can be seen even more clearly in the inset of Fig. 2 which represents a magnification of Fig. 1(c). In analogy

to solitonic water waves that run through other waves without loosing their shape, we call the states that correspond to these levels *solitonic* states. Those eigenstates should not be considered as solitons propagating in *real space*, they rather propagate through the irregular bulk of energy levels evolving with a fictitious time, namely the tilting strength [20]. In the rest of the paper we are going to investigate both the properties of the solitonic states as well as the mechanism generating them.

We begin the discussion with the case of vanishing tunneling $J = 0$ (see Fig. 1(a)). Then, the BHH (1) commutes with the center-of-mass operator $\sum_{l=1}^{M} \tilde{l}\hat{n}_l$. As a result, the eigenstates are independent of the tilt F and are given by the Fock states $|n_1, n_2, \ldots, n_M\rangle$, i.e. states with a well-defined number of atoms per site. The eigenenergies, in turn, depend exactly linearly on the tilting strength F (with a proportionality factor given by their center of mass) and undergo level crossings. For vanishing tilt the eigenenergies equal the inter-atomic interaction energy and thus all configurations of particles in which the same number of particles share a lattice site are energetically degenerated. In Fig. 1(a) the upper set of levels (we say manifold) corresponds to the states where all N particles are located on one site. Descending in energy one finds the manifolds corresponding to states with $N-1, N-2, \ldots, 1$ particles on one site. Accordingly, for $F = J = 0$ the number of different eigenenergies is given by N, the number of particles in the system. For finite tilt F the degeneracy is partially lifted and Fock states with different values of the center of mass are energetically separated. We note that as the levels cross with increasing F, the energetical ordering according to the site occupation is no longer valid.

As anticipated above, the expectation value of the center of mass in the BHH is the level velocity:

$$\frac{\partial E_n(F)}{\partial F} = \langle \Psi_n | \sum_{l=1}^{M} \tilde{l}\hat{n}_l | \Psi_n \rangle. \tag{2}$$

Thus, the level velocity (slope) immediately reveals where on the lattice a given state is located. For example in the upper manifold in Fig. 1(a) the level with the most negative gradient corresponds to all particles being localized on site $l = 1$ while the next higher level has all particles localized on site $l = 2$ and so on. Since (2) is valid for arbitrary tunneling it can be used in the following to identify Fock-like states also for finite tunneling: if the gradient of a state is similar to the gradient of the Fock state with all particles at the boundary of the lattice (steepest slopes), then the states also must be Fock-like.

As the tunneling is increased to $0 < J \ll U$ (see Fig. 1(b)), one observes that many degeneracies are lifted already at $F = 0$. This is pronounced most strongly for states with intermediate or low energies $E \lesssim 0.05$. But interestingly, there is hardly any influence of the finite tunneling rate on the manifold of levels with the highest energy which still are very similar to Fock states with all particles localized at one site. In analogy with the repulsively bound pairs mentioned in the introduction [7], one could argue that the regularity of these states results from the energy gap between the upper and the lower part of the spectrum, representing a strongly non-resonant transition. However, the apparent regularity persists even as the states of this manifold have submerged in the chaotic bulk of the spectrum and energy separation does not explain why the corresponding levels keep their linear shape after transitions to other states become resonant.

A further increase of the tunneling strength $J \approx U$ (see Fig. 1(c)) leads to the predominantly chaotic regime. Indeed, one observes that basically all degeneracies are now lifted and the levels exhibit *avoided* crossings. On the one hand, the larger tunneling term should lead to a F-dependence of the eigenstates and, on the other hand, it should "delocalize" also the regular states from the upper manifold. In contrast, we find by direct inspection of Fig. 1(c) that for these solitonic states the linear F-dependence persists. Compared with the generically strong coupling between the majority of the chaotic levels, their coupling to the solitonic states is weak (the resulting small avoided crossings are shown in the inset of Fig. 2). In accordance with this weak coupling, none of the crossings leaves a trace in the slope of the solitonic states on a larger scale. Summarizing we can now asset that we observed regular structures in the chaotic bulk of the energy spectrum that are not due to energetic isolation and even survive an enhanced tunneling strength. In the next section we will characterize the solitonic states.

Solitonic states Before entering the detailed analysis we first note that the energetically lowest lying solitonic state from the upper manifold in Fig. 1(c) has a very large negative gradient and hence should be Fock-like (see above). In addition, the linear dependence of all solitonic states indicates that the center-of-mass operator is a constant of motion for this part of the state space. In fact, in the following we will give evidence that the solitonic states are highly localized both in the Fock basis and on the lattice itself.

We begin with the description of the solitonic states in the Fock basis. In Fig. 2 we show for an exemplary value of the tilt ($F = 0.002$) the modulus squared of the expansion coefficients $|c_i|^2$ in the Fock basis of the above mentioned solitonic state (red) and for a typical chaotic state (black). While in the latter case many basis states are occupied, the solitonic state has only very few non-vanishing components $|c_i|^2$ and hence the overlap with the chaotic state is very small. A closer look at the $|c_i|^2$ of the solitonic state reveals that the largest coefficients correspond to Fock states where all particles are located on a single lattice site; In this case

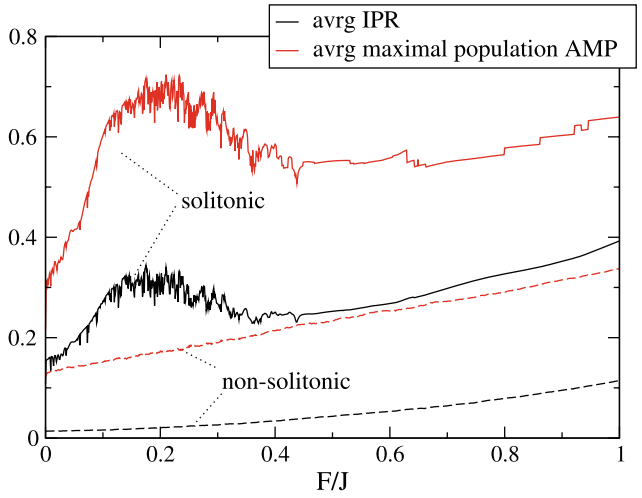

Fig. 3 Average IPR (see (3)), of the eigenstates of the BHH (1), in the Fock basis (*black lines*) and average maximal population AMP (see (4)) on a single lattice site normalized with the number of particles (*red lines*). The *solid lines* correspond to the average of the $M = 11$ eigenstates with the largest IPR, the *dashed lines* to the average of all the other eigenstates. The parameters are chosen as in Fig. 1(c)

the maximal is $|c_i|^2 \sim 0.7$ and corresponds to all particles on the site $l = 1$.

In order to quantify and to extend this observation for arbitrary tilt F we introduce the inverse participation ratio (IPR), which is defined as

$$\mathrm{IPR}\big(|\psi\rangle\big) = \sum_{i=1}^{\mathcal{N}} |c_i|^4, \tag{3}$$

where the c_i are the expansion coefficients of the state $|\psi\rangle$ in the Fock basis. The IPR takes the limiting values one for basis states, and $1/\mathcal{N}$ for a superposition of all basis states with same weight, where $\mathcal{N}$ is the Hilbert-space dimension. Therefore, the IPR represents the inverse number of basis states that are occupied by the state $|\psi\rangle$. We have found that (apart from the vicinity of an avoided crossing) over a large range of F the solitonic states correspond to the states of the highest IPR. A quantitative comparison between the IPRs of solitonic (solid black line) and non-solitonic states (dashed black line) is shown in Fig. 3 where we average over the solitonic levels on the one hand and over all remaining non-solitonic states on the other hand. The localization of the solitonic states is manifest in the IPR-enhancement of about an order of magnitude as compared to the non-solitonic states. The average IPR of the latter states depends only weakly on the tilt F, but the slight increase with growing F shows the onset of Stark localization which is expected for large tilts [19]. The solitonic states on the other hand, do not show this monotonic behavior. Besides the fluctuations, that are a consequence of the small sample of solitonic states, there is an increase for $F/J \lesssim 0.15$, followed by a plateau for $0.15 \lesssim F/J \lesssim 0.35$, and a subsequent decrease of the IPR for $F/J \gtrsim 0.35$. Finally the curve increases in a weaker manner for $F/J \gtrsim 0.5$. An increase for $F/J \lesssim 0.15$ is in agreement with the expected formation of well-localized Wannier–Stark states for growing F. However, the comparison with the behavior of the non-solitonic states—that show a significantly smaller increase—raises doubts whether this is indeed the correct explanation. Additionally, the IPR decreases for $F/J \gtrsim 0.35$ before rising again, indicating that the solitonic states are not simply a result of Stark localization.

Next, we focus on the localization of the solitonic states on the lattice. The above analysis of the Fock basis components (see Fig. 2) indicates that the largest coefficients $|c_i|^2$ correspond to states where all particles are localized on a single site. Additionally, we observed that the other non-vanishing coefficients belong to Fock states with a similar center of mass. If, for example, the soliton has a large overlap with the Fock state $|N, 0 \ldots\rangle$, then there is also a finite overlap with $|N-1, 1, 0, \ldots\rangle$ while Fock states with strongly different center of mass are not occupied. Hence, we conclude that the solitons are highly localized on the lattice itself.

In order to quantify the localization of the state on the lattice we use the average maximal population (AMP) on a single site. This quantity is the average over all solitonic or non-solitonic states of the largest occupation $\langle\psi|\hat{n}_l|\psi\rangle$ of the M different sites, normalized by the number N of particles:

$$\mathrm{AMP} = \left\langle \frac{\max_l \langle\psi|\hat{n}_l|\psi\rangle}{N} \right\rangle. \tag{4}$$

The maximum value of unity corresponds to the configuration in which all N particles are located on a single site. The results are depicted as red (dashed) lines for the (non-)solitonic states in Fig. 3. In contrast to the non-solitonic states, typically more than 60% of all atoms in a solitonic state are located on a single site. This supports the claim that there are as many solitonic states as there are lattice sites M which is also in agreement with the parametric level evolution and can be seen in Fig. 1, where the system consists of 11 sites and 11 solitons are found.

Although both measures show the same dependence on the external parameter (in this case the tilt F), the AMP provides a clear physical interpretation of the solitonic eigenstates. They are not merely some particular Fock states but they are localized on a specific site of the lattice and they hardly change their location under changes of the tilt, what defines a clear experimental evidence of them and also allows to understand the underlying mechanism for their appearance that we discuss in the following.

Mechanism The transition amplitude from an initial state $|\Psi_I\rangle$ to a final state $|\Psi_F\rangle$ under a change in the lattice tilt is given by $\langle\Psi_F|\sum_{l=1}^{M} \tilde{l}\hat{n}_l|\Psi_I\rangle$, i.e. the corresponding matrix element of the center-of-mass operator. As seen above, the solitonic states are distinguished by the fact that virtually all atoms are occupying the same lattice site, what is in contrast to the chaotic states for which the atoms are distributed over the entire lattice. Because of their strong localization the solitonic states are approximate eigenstates of the center-of-mass operator. Therefore, the amplitude for a transition from a solitonic to a chaotic state is essentially proportional to the overlap between these two states, which, in turn, vanishes since both are system eigenstates. More intuitively, a transition from a solitonic to a chaotic state requires the redistribution of essentially all atoms over the entire lattice. The tunneling of an atom over more than a single lattice site and simultaneous tunneling of more than one atom, however is negligible for typical lattice-depths and is not taken into account in the Bose–Hubbard Hamiltonian (1).

But there also exist system eigenstates that are very well approximated by all but one atoms located on a single site and the remaining particle localized to some other site. These states show similar features as the solitonic states described so far and will be referred to as solitonic states of second order. Since tunneling of a single atom over a single site only is necessary for a transition from a solitonic state of first order to a solitonic state of second order, one might expect significantly larger transition amplitudes as compared to transitions to chaotic states. These transitions, however, are strongly suppressed for energetic reasons: the energy difference between a solitonic state of first order and a solitonic state of second order that results from the first order state by a single tunneling event amounts to $U(N-1)-F$; due to the localization of solitonic states their tunneling energy is negligible. Thus, transitions are energetically allowed if the tilt strength F is $N-1$ times larger than the interaction energy, which is far outside the regime in which solitonic states exist, as discussed for the IPR and seen in Fig. 3. Given the linear increase of the difference in the interaction energy $U(N-1)$ with the particle number N, the energetic stabilization of the solitons becomes even more pronounced with increasing particle number. The same holds also for the suppression of transitions from solitonic to chaotic states: the more particles are participating in a solitonic state, the more particles have to undergo tunneling processes in order to realize a chaotic state. Therefore, the stability of solitonic states is expected to be enhanced with increasing number of particles. In our studies, we have verified that solitonic states also appear for larger boson numbers and even for filling factors N/M larger than one. However, for solitonic states with an increasing number of particles located on a single site, three-body interactions (that are not described by the BHH) can become a non-negligible effect. Such three-body collisions may result in additional decay channels [15] for solitonic states, which eventually can set limits to the maximum number of atoms participating in such a state.

Summary In summary, we have analyzed the spectrum of the Bose–Hubbard Hamiltonian in the predominantly chaotic regime as an external parameter—in this case a static field (tilt)—is varied. We have found that despite the chaoticity there exist regular structures in the spectrum, that exhibit a simple linear dependence on the external parameter. The associated eigenstates are the *solitonic states* that retain their shape during the change of the tilt. We have shown that the robustness of these states is neither due to Stark localization nor to an energetic isolation [7] but is induced by the interplay of interaction and single-particle dynamics. The solitonic states are characterized by a strong localization on the lattice and by their weak coupling to the non-solitonic levels. The former property represents an appealing signature for their experimental detection in terms of modern microscopy techniques in optical lattices [21]. The latter property makes solitonic states excellent candidates for coherent control, since—in contrast to basically all the non-solitonic states—they are insensitive to (small) changes in the external conditions. Specifically, we expect that this robustness of the solitonic states becomes particularly manifest in a *dynamical* evolution where, for example, the lattice is driven non-adiabatically by sweeping its tilt.

Acknowledgements We acknowledge support of the Deutsche Forschungsgemeinschaft DFG via the *Forschergruppe* 760 and the Grant MI1345/2-1. B.O. gratefully acknowledges financial support of the European Science Foundation within the QUDEDIS program, Marie Curie ToK project COCOS (MTDK-CT-2004-517186) and of the Polish Government (scientific funds 2008–2011).

References

1. I. Bloch, J. Dalibard, W. Zwerger, Rev. Mod. Phys. **80**, 885 (2008)
2. O. Morsch, M. Oberthaler, Rev. Mod. Phys. **78**, 179 (2006)
3. M. Lewenstein, A. Sanpera, V. Ahufinger, B. Damski, A. Sen, U. Sen, Adv. Phys. **56**, 243 (2007)
4. M. Greiner, O. Mandel, T. Esslinger, T.W. Hänsch, I. Bloch, Nature **415**, 39 (2002)
5. W. Zwerger, J. Opt. B **5**, S9 (2003)
6. D. Jaksch, C. Bruder, J.I. Cirac, C.W. Gardiner, P. Zoller, Phys. Rev. Lett. **81**, 3108 (1998)
7. K. Winkler, G. Thalhammer, F. Lang, R. Grimm, J.H. Denschlag, A.J. Daley, A. Kantian, H.P. Buchler, P. Zoller, Nature **441**, 853 (2006)
8. S. de Filippo, M. Fusco Girard, M. Salerno, Nonlinearity **2**, 477 (1989)
9. A. Chefles, J. Phys. A **29**, 4515 (1996)
10. A.R. Kolovsky, A. Buchleitner, Europhys. Lett. **68**, 632 (2004)
11. M. Hiller, T. Kottos, T. Geisel, Phys. Rev. A **73**, 061604(R) (2006)
12. A.J. Lichtenberg, M.A. Lieberman, *Regular and Chaotic Dynamics* (Springer, New York, 1992)
13. B.V. Chirikov, Phys. Rep. **52**, 263 (1979)

14. F. Dalfovo, S. Giorgini, L.P. Pitaevskii, S. Stringari, Rev. Mod. Phys. **71**, 463 (1999) dNLS16
15. A.J. Leggett, Rev. Mod. Phys. **73**, 307 (2001)
16. S. Inouye, M.R. Andrews, J. Stenger, H.-J. Miesner, D.M. Stamper-Kurn, W. Ketterle, Nature **392**, 151 (1998) dNLS125
17. A.R. Kolovsky, A. Buchleitner, Phys. Rev. E **68**, 056213 (2003)
18. M. Hiller, T. Kottos, T. Geisel, Phys. Rev. A **79**, 023621 (2009)
19. A. Buchleitner, A. Kolovsky, Phys. Rev. Lett. **91**, 253002 (2003)
20. J. Zakrzewski, A. Buchleitner, D. Delande, Z. Phys. B **103**, 115 (1997)
21. W.S. Bakr, J.I. Gillen, A. Peng, S. Folling, M. Greiner, Nature **462**, 74 (2009)